Research Article

Investigation of the microstructure, hardness, and compressive properties of TaC-reinforced lamellar graphite cast irons

Rifat Yakut[1*], Ömer Çiftçi[2]

[1]Department of Energy Systems Engineering, Batman University, Batman, Turkey
[2]Department of Mechanical Engineering, Batman University, Batman, Turkey

ORCID: R. Yakut (0000-0003-0059-3785), Ö. Çiftçi (0000-0003-0500-7730)

Abstract: Tantalum Carbide (TaC) reinforcement was made to lamellar graphite cast irons that were produced at reinforcement ratios of 0%, 0.025%, 0.155%, and 0.285% in the physical conditions of a foundry. Samples complying with standards were prepared using the TaC-reinforced lamellar graphite cast iron alloys that were produced. Brinell hardness tests, compressive strength tests, and microstructural analyses were conducted on these samples. According to the test results, the highest average Brinell hardness value was found as 231 HB in sample A that was reinforced at a ratio of 0.025%. In general, as the reinforcement ratio increased, there was an increase in the hardness test measurement results. The highest average compressive strength value was found as 949 MPa in sample C that was reinforced at a ratio of 0.285%. In general, as the reinforcement ratio increased, there was an increase in the compressive strength values. The results of the microstructural analyses showed that the reinforcement material was dispersed into the matrix.

Keywords: Lamellar Graphite Cast Iron, Gray Cast Iron, Tantalum Carbide (TaC), Sand Casting

1. Introduction

The group of iron materials that contain more than 2% carbon in their chemical composition is called cast irons [1]. Cast irons are iron-carbon-silicon alloys. They contain approximately 2-4% C and 1-3% Si. In addition to carbon and silicon, they also contain elements such as manganese, phosphorus, and sulfur. Because the final shapes and dimensions of these materials can be achieved by the method of casting, they are called cast iron materials. They are used in a wide range of applications and have varying properties of strength, corrosion resistance, hardness, wear resistance, easy machinability, and vibration dampening [1-3]. Additionally, cast iron materials also have many advantageous properties such as the inexpensiveness and easiness of the melting process, good fluidity, low melting points, and thermal conductivity. These superior properties of cast irons allow them to be prevalently used in several structural applications and the automotive industry [4, 5].

Cast irons are conventionally used in many industrial applications due to their usage flexibility, good castability, low costs (20-40% lower than steel), and a highly variable selection of mechanical properties [6]. The properties of cast irons include combinations of good mechanical properties, physical properties, and economical manu-

facturing processes [7, 8]. The fact that the melting temperature of cast irons is approximately 1600°C makes them practical for industrial applications [9]. High carbon ratios in cast irons lead to higher brittleness values. In practical applications, cast irons are known as Fe-C-Si (iron, carbon, and silicon) alloys that contain up to 3.5 silicon and up to 4.4% carbon [10-12]. In addition to these elements, manganese and lower ratios of sulfur and phosphorus can also be encountered [13]. The separation of carbon during solidification appears as a separate element in the microstructures of cast iron materials. The shape and composition that is formed with the revelation of carbon during solidification determine the types of cast iron materials, therefore affecting their properties [10].

The first development in the manufacturing of cast iron materials was the production of lamellar graphite cast irons (gray cast irons) by the implementation of the inoculation method [14]. At the stages before the pouring process, the structure of lamellar graphite (gray) cast irons is dependent on the cooling conditions, inoculants, and chemical compositions [6]. In the automotive industry, lamellar graphite (gray) cast iron materials are frequently used in the production of blocks, brake drums and disks, engines, piston rings, cylinder heads, and cyl-

Table 1. Chemical compositions of the samples (%)

No	C	Si	Mn	P	S	Cr	Cu	Al	Ti	TaC
A	3.36	2.68	0.68	0.006	0.067	0.28	0.08	0.001	0.033	0.025
B	3.38	2.70	0.64	0.017	0.083	0.28	0.12	0.001	0.033	0.155
C	3.23	2.71	0.63	0.016	0.086	0.28	0.12	0.001	0.025	0.285
K	3.30	2.70	0.63	0.016	0.080	0.28	0.12	0.001	0.025	-

inder linings [4, 5, 7, 8]. In this study, Tantalum Carbide (TaC) was added at different ratios (sample K: 0%, sample A: 0.025%, sample B: 0.155%, and sample C: 0.285%) to lamellar graphite cast irons that are prevalently use in the industry, and these samples were subjected to compressive tests, hardness tests, and microstructural analyses.

2. Material and Method

2.1. Material Production
The casting samples to be used in this study were produced using the sand-casting method in the conditions of the foundry of the Casting Factory of the firm Hema Otomotiv at a final pouring temperature of 1375°C by the addition of tantalum carbide (TaC). The lamellar graphite cast iron materials that were produced were subjected to microstructural analyses, compressive strength tests, and hardness tests. Lamellar graphite (gray) cast irons are classified based on the ASTM A 48 standard [15]. The chemical compositions of the samples are shown in Table 1 [3, 16].

During the pouring process of the sample materials, inoculation material was added at a ratio of 0.3% by weight. The chemical composition of the inoculation material is given in Table 2.

2.2. Reinforcement Material
The TaC reinforcement material to be used in this study was obtained from the firm Nanografi Nano Teknoloji. TaC is a very hard and brittle material that has an electrical conductivity value similar to that in metals [17]. The mechanical properties of the TaC that was used in this study are shown in Table 3 [18].

2.3. Preparation of Test Samples
After pouring, the lamellar graphite cast iron samples were removed from their sand molds at room temperature. From these samples, hardness test samples at the dimensions of 30x30x50 mm were obtained. Brinell hardness measurements were taken from 5 points in different zones on the surface of each sample, and the averages of these 5 measurements were determined in all samples. This way, the average hardness values of the samples were obtained. Among the hardness test samples, the appearance of sample A is shown in Figure 1. The hardness measurements were made in compliance with standards using an Ernst AT250DR brand Brinell hardness measurement device. The reason for using the Brinell hardness measurement method in this study was

the fact that it leaves deeper and broader traces on the surface of the material in comparison to other hardness measurement methods. This way, the hardness values of a broader area on the surfaces of the measured samples can be obtained. To compare the results of the samples that were subjected to hardness tests, the measurement conditions were kept similar.

In gray cast irons, following solidification, a large part of the carbon in the composition is found in the form of free graphite flakes (lamellar structures). When these materials are broken, their surface has a gray appearance. This is why they are called gray cast irons. They are also known as lamellar graphite cast irons [19]. Lamellar graphite cast irons are alloys that are close to a eutectic composition. This is why their viscosity properties are highly favorable. For this reason, it is possible to cast parts with thin cross-sections. The compressive strength of lamellar graphite cast irons is approximately 3-5 times their tensile strength. This high compressive strength is one of the important properties of lamellar graphite cast irons. In these cast irons, hardness measurement values and tensile strength measurement values show parallelism [14].

In terms of the procedure, compressive strength tests are considered the opposite of tensile strength tests. Compressive strength tests are usually applied on brittle materials that are expected to be exposed to compressive loads. Because the compressive strength values of metal materials such as bearing alloys produced from lamellar graphite (gray) cast irons are higher than their tensile strength values, such materials are used at places of ex-

Table 2. Chemical composition of the inoculation material (%)

	Si	Al	Ca	Sr
Min-Max	73.0-78.0	0.50 max	0.100 max	0.80-1.40
Sample Castings	75.0	0.32	0.020	1.06

Table 3. Technical properties of TaC

Purity	99.9 %
Particle Size	~3 μm
Melting Point	3880 °C
Boiling Point	5500 °C
Density	13.9 g/cm³
Form	Powder
Mohs Hardness @ 20ºC	1800 kg/mm²
Electric Resistivity	30 microohm-cm
Crystal Structure	Cubic

posure to compressive stresses, and they are evaluated by compressive strength tests [20]. In compressive strength test samples, it is recommended that the dimensional ratio (initial height (h_0) to initial diameter (d_0)) be $1.5 \leq h_0/d_0 \leq 10$. In the compressive strength testing of metallic materials, this ratio is usually taken as $h_0/d_0=2$. If the h_0/d_0 ratio of samples is too high, distortions and non-homogeneous stress distributions can be observed in the samples during testing. If the h_0/d_0 ratio is too low, the friction between the sample and the compression heads influences the experimental results substantially [21]. For the compressive strength tests in this study, cylindrical samples at the dimensions of Ø12 mm x 19.2 mm were prepared. The tests included a total of 12 samples, 3 samples for each reinforcement ratio (Figure 2). Among the compressive strength test samples, sample C is shown in Figure 2. The samples were tested in compliance with the ASTM E9 standard using a Zwick Roell Z600 universal testing device at a ratio of $h_0/d_0=1.6$ and a strain rate of 0.5 mm/min. To compare the results of the samples that were subjected to compressive strength tests, the measurement conditions were kept similar.

For metallographic analyses, the samples were cut at the dimensions of 15x15x15 mm. The tests included a total of 12 samples, 3 samples for each reinforcement ratio. The samples were obtained using a Metkon METACUT 250 brand precision cutting machine. To make the following procedures more practical, the cut samples were mounted in Bakelite in 4 batches. Each Bakelite set included 3 samples. The Bakelite mounting process was carried out using a Metkon ECOPRESS 50 device. The samples that were cut and mounted in Bakelite were subjected to sanding and polishing for the imaging procedures. Sanding and polishing were applied to eliminate problems that would affect the images negatively such as scratches on the surface. The samples were sanded using 120-, 240-, 400-, 800-, and 1200-grit sandpapers, respectively. After sanding, the polishing process was carried out on

Figure 1. Sample A for hardness measurements

Figure 2. Sample C for compressive strength measurements

a haircloth with 1% diamond polish and lubricant, and the samples were made ready for etching. These procedures were carried out using a Metkon FORCIPOL 2V device. Etching was performed using a 3% Nital solution. The samples were submerged into the etching solution and kept in the solution for 5 seconds to prepare them for optical microstructural analyses. A Nikon MA 100 brand metal optical microscope (OM) was used to take microstructural images, and the Clemex system was preferred for imaging. For the metallographic examinations, a Tescan MAIA3 XMU brand scanning electron microscope (SEM) was used.

3. Result and Discussion

3.1. Hardness Test Results

According to the information in the relevant literature, the mechanical properties of cast irons vary depending on graphite morphology (shape, distribution, quantity, and particle size) and matrix structures (ferrite, pearlite). It was shown that an increase in the ratio of pearlite in the matrix structure and the homogeneous distribution on graphite morphology increase hardness values [22]. While cast irons display a wide range of mechanical/physical properties, they usually have hardness values of 120-300 HB, and these values can reach 600 HB in special wear-resistant cast irons [13]. Akgül (2018) determined the Brinell hardness values of unreinforced lamellar graphite (gray) cast iron as 145 HB [22]. Çalık et al. (2022) measured the Brinell hardness values of GG-25 gray (lamellar graphite) cast iron samples that were produced using the centrifugal casting and sand-casting methods. According to their measurements, the authors found the average outer surface hardness value of the samples that were produced by sand-casting as 212 HB and the average outer surface hardness value of the samples produced by centrifugal casting as 255 HB [23].

The hardness measurement tests of this study were carried out in compliance with the methods reported in the relevant literature. The average of the measurement results of each sample was taken, and the results of the samples were compared to the results of previous studies conducted on lamellar graphite cast irons. As a result of the comparisons, it was determined that the hardness test results were compatible with those in the literature. In the tests, the lowest hardness value was found as 224 HB in the unreinforced sample K. As expected, due to the higher reinforcement ratio, the hardness value of sample A was 231 HB, which was higher than that of sample K. Although the reinforcement ratio increased in sample B, its hardness value (avg. 225 HB) was greater than the hardness value of sample K but lower than that of sample A that had a lower reinforcement ratio. The reason for this may be that because the pearlitic structure affects the material's hardness significantly, a more pearlitic microstructure would increase the hardness of the material in direct proportion. A less pearlitic microstructure, on the other hand, would reduce the hardness of the material proportionally [13]. Another increase was seen in sam-
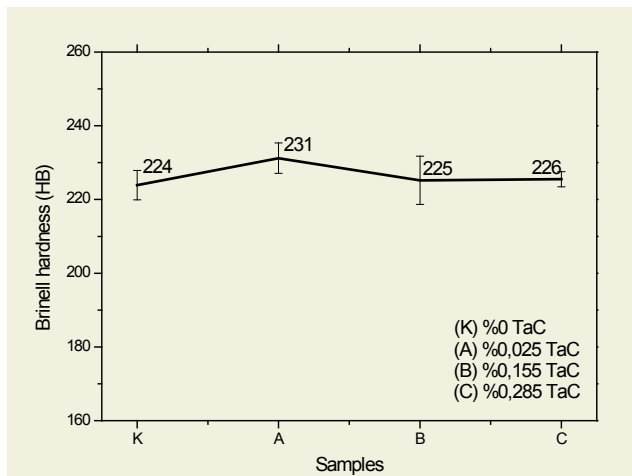
Figure 3. Brinell hardness measurement values
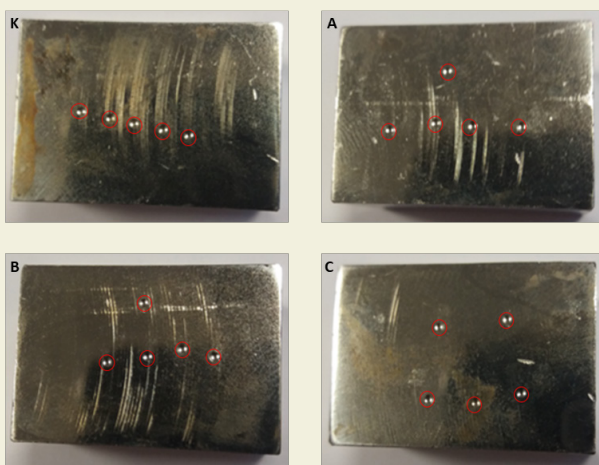
Figure 4. Appearance of surfaces on which Brinell hardness measurements were made

values of lamellar graphite cast irons are approximately 3-5 times their tensile strength values [19]. Based on the information in the literature, considering values 3 times as large as their expected tensile strength (100-350 MPa), their expected compressive strength values would be in the range of 300-1050 MPa.

To be able to compare the results of the compressive strength tests among the samples, the tests of all samples in the study were carried out under the same conditions. It was determined that the results of the compressive
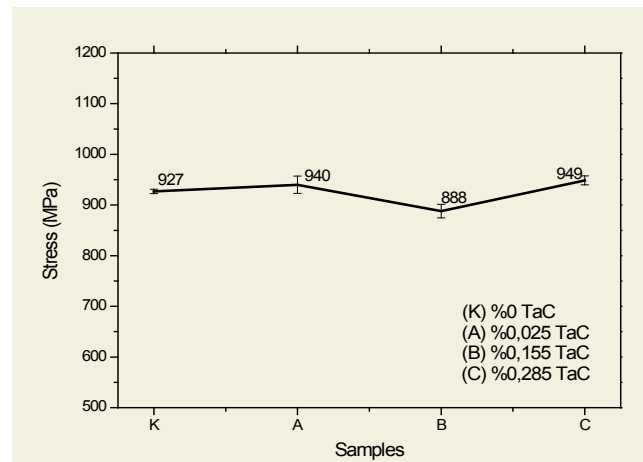
Figure 5. Compressive strength measurement values
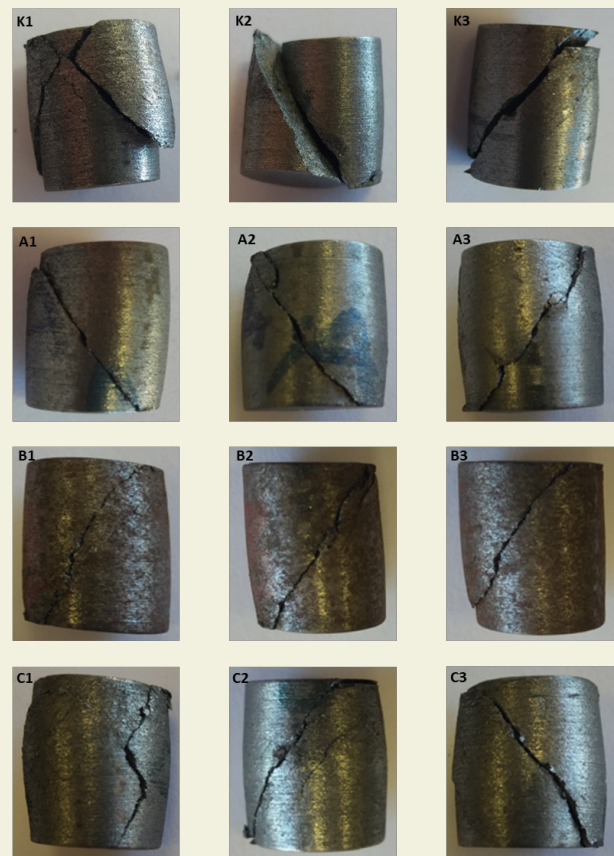
Figure 6. Appearance of strain failures in the compressive strength tests

ple C, which had an average hardness value of 226 HB. Among all values, the highest average hardness value was found in sample A. While the Brinell hardness measurement values of the samples depending on their reinforcement ratios are given in Figure 3, the appearance of sample surfaces on which hardness measurements were made is shown in Figure 4.

3.2. Compressive Strength Test Results

Compressive strength tests are usually applied to brittle materials that are expected to have higher compressive strength values than their tensile strength values. The compressive strength values of lamellar graphite (gray) cast irons vary depending on their matrix structures and their graphite flake sizes, types, and distributions. During solidification, it is desired that the flakes are randomly dispersed, and smaller type-A flakes are formed [14]. In this study, it was observed that the graphite flakes were not dispersed in one direction, they were randomly distributed, and their lamellar form was type-A. While determining the compressive strength of gray cast irons, their tensile strength is taken into account. The tensile strength values of gray cast irons are typically in the range of 100-350 MPa [24]. The compressive strength

Figure 7. Compressive strength test stress-strain plots

strength tests in this study were compatible with those in the literature. In the tests, the average compressive strength value of the unreinforced sample K was found as 927 MPa. As the reinforcement ratio increased, there was an increase in the compressive strength values, and the average compressive strength value of sample A was found as 940 MPa. It was expected that the compressive strength values would increase along with the increasing reinforcement ratios. However, although the reinforcement ratio of sample B was higher, there was a decrease in its compressive strength (avg. 888 MPa). This result was in parallel with the result observed in the hardness tests. This result may be explained by the pearlitic microstructure as in the case of the hardness tests and the possibility that the strength values decreased due to the creation of an unpredictable notch effect in the flakes in the matrix caused by stresses [13, 22]. In compliance with expectations based on the reinforcement ratios and ma-

terial properties, in sample C, the compressive strength values increased, and the average value was found as 949 MPa. The highest average compressive strength value was determined in sample C, which also had the highest reinforcement ratio. The compressive strength values of the samples depending on the reinforcement ratios are given in Figure 5.

Looking at the stress-strain plots of the compressive strength tests, while the curves were similar to each other, it was seen that there were differences in the yield points, the highest stress points, and the fracture points. When the stresses caused by the compressive loads that were applied reached a certain value, strain failure occurred due to the notch effect created by the flakes in the microstructure (Figure 6). The stress-strain plots of the compressive strength tests are shown in Figure 7.
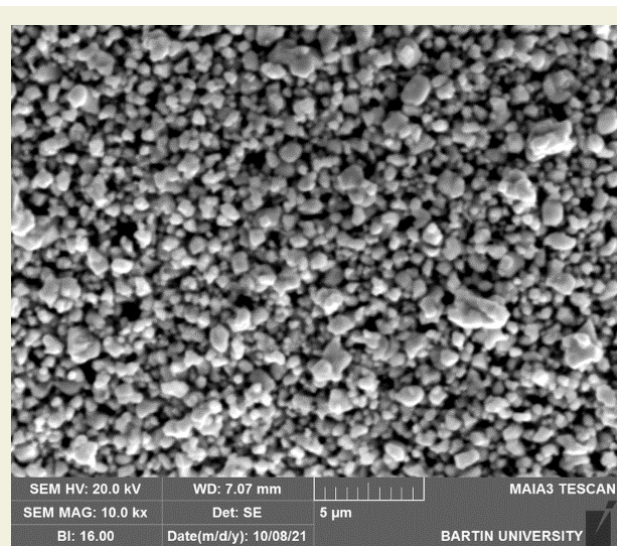
Figure 8. SEM image of the TaC powder
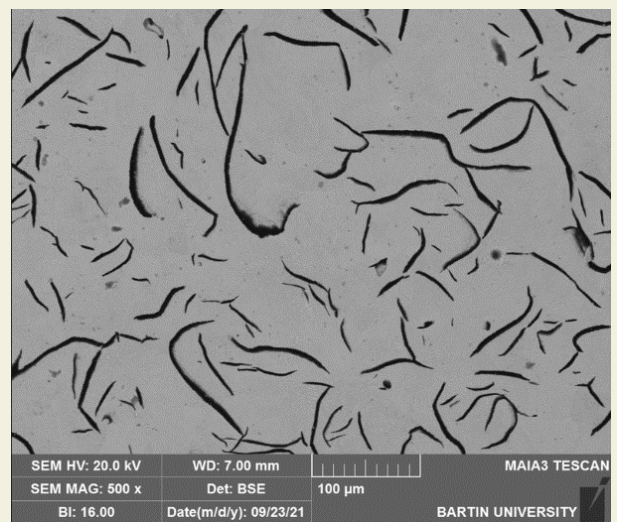
Figure 9. SEM image of the microstructure (sample A)
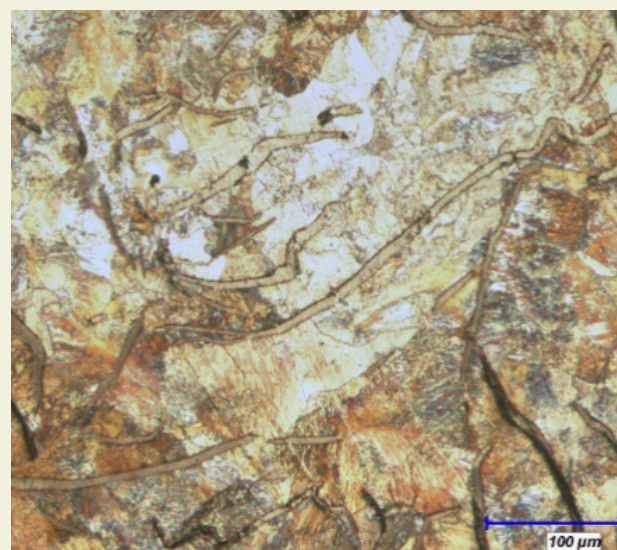
Figure 10. OM image of the microstructure (sample A) (20X)

3.3. Microstructure Analysis Results

The SEM image of the TaC powder that was used as a reinforcement material is shown in Figure 8, the SEM microstructure image of sample A is shown in Figure 9, and the OM microstructure image of sample A is shown in Figure 10.

The microstructure of lamellar graphite cast irons is in the form of graphite flakes dispersed in the iron matrix. The process at a foundry affects the nucleation and growth of graphite flakes, and thus, the sizes and forms of the flakes can be used to achieve the desired casting outcomes. Graphite ratios, sizes, morphology, and graphite flake distributions are critically important in the determination of the mechanical behaviors of lamellar graphite cast irons [23]. An EDS analysis was conducted from the marked region of sample A (Figure 11), and the results revealed 2.2% silicon (Si), 21.2% iron (Fe), 27.4% carbon (C), and particularly, 49.1% tantalum (Ta).

4. Conclusion

In this study, the microstructure, hardness, and compressive strength behaviors of lamellar graphite (gray) cast irons in which TaC reinforcement was added at different reinforcement ratios were investigated, and the ob-
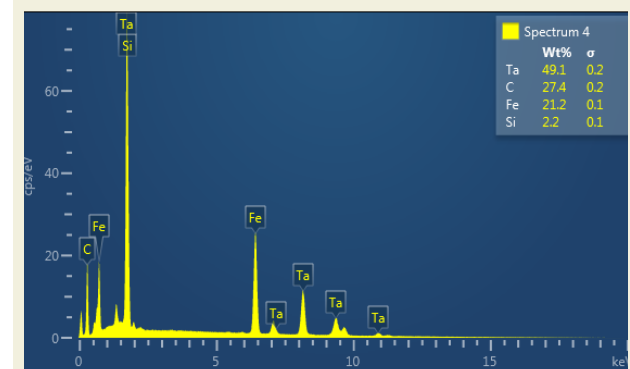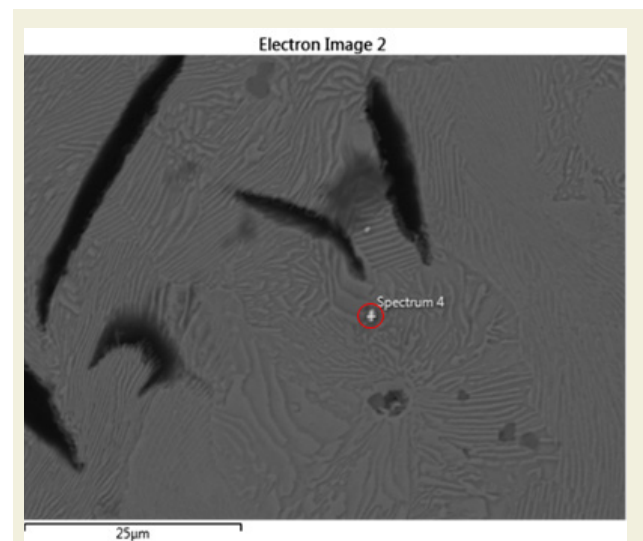
Figure 11. EDS analysis results (sample A)

tained results are presented below.

- In the hardness measurements, the highest hardness value was obtained in sample A as 231 HB. In comparison to the unreinforced sample K, the hardness values of samples A, B, and C were higher. In parallel with the literature, hence, it was observed that hardness increased along with increasing reinforcement ratios.

- In the compressive strength measurements, the highest compressive strength value was obtained as 949 MPa in sample C, which had the highest reinforcement ratio. In general, it may be stated that compressive strength values increased along with increasing reinforcement ratios.

- According to the microstructural analysis results, the TaC reinforcement material was dispersed into the chemical composition of the lamellar graphite cast iron material.

- The microstructural analyses showed that the graphite flakes were randomly dispersed in the iron matrix.

References

[1] Çolak, M., Arslan, İ., & Gavgalı, E. (2018). Solidification simulation of gray cast iron and comparision with real cast. Engineering Sciences (NWSAENS), 13 (4): 280-290, DOI: 10.12739/NWSA.2018.13.4.1A0419.

[2] Münker, F. (2010). Wear properties of hardened cast irons. Master Thesis, Marmara University, Graduate School of Natural and Applied Sciences, İstanbul.

[3] Çiftçi, Ö., & Yakut, R. (2021). Effects of TaC addition to lamellar graphite cast irons on mechanical properties. International Cappadocia Scientific Research Congress, 15-17 December, Cappadocia-Nevşehir, p. 107-113.

[4] Malcıoğlu, A. U. (2015). Investigation of wear behaviour of austempered gray cast iron at elevated temperature. Master Thesis, Istanbul Technical University, Graduate School of Natural and Applied Sciences, İstanbul.

[5] Diószegi, A., Svidró, P., Elmquist L., & Dugic, I. (2016). Defect formation mechanisms in lamellar graphite ıron related to the casting geometry. International Journal of Cast Metals Research, 29 (5): 279-285, DOI:10.1080/13640461.2016.1211579.

[6] Collini, L., Nicoletto, G., & Konecna, R. (2008). Microstructure and mechanical properties of pearlitic gray cast iron. Materials Science and Engineering A, 488 (1-2): 529-539, DOI: 10.1016/j.msea.2007.11.070.

[7] Bilici, M. K. (2004). Wear properties of an alloy cast iron. Master Thesis, Marmara University, Graduate School of Natural and Applied Sciences, İstanbul.

[8] Ghasemi, R., & Elmquist, L. (2014). A study on graphite extrusion phenomenon under the sliding wear response of cast iron using microindentation and microscratch techniques. Wear, 320 (2014): 120-126, DOI: 10.1016/j.wear.2014.09.002.

[9] Beniwal, G., & Saxena, K. K. (2020). Effect of niobium addition in grey cast iron: A short review. Materials Today: Proceedings, 26 (2): 2337-2343, DOI: 10.1016/j.matpr.2020.02.503.

[10] Aytaçoğlu, L. C. (2012). Thermal analysis of cast iron and mathematical approach to thermal analysis. Master Thesis, Sakarya University, Graduate School of Natural and Applied Sciences, Sakarya.

[11] Lima, F. F. O., Bauri, L. F., Pereira H. B., & Azevedo, C. R. F. (2020). Effect of the cooling rate on the tensile strength of pearlitic lamellar graphite cast iron. International Journal of Cast Metals Research, 33 (4-5): 201-217, DOI: 10.1080/13640461.2020.1822573.

[12] Aguado, E., Ferrer, M., & Larranaga, P. (2019). The effect of the substitution of silicon by aluminum on the properties of lamellar graphite ıron. International Journal of Metalcasting, 13 (3): 536-545, DOI: 10.1007/s40962-018-00303-y.

[13] Şen, N. B. (2018). The investigation of the mechanical, metallurgical and economic effect of metallurgical silicium carburete and ferro silicon additives on the materials of production of lamel graphite cast iron. Master Thesis, Necmettin Erbakan University, Graduate School of Natural and Applied Sciences, Konya.

[14] Kurt, B. (2019). Investigation of the effect of carbon equality on microstructure and mechanical properties with thermal analysis methods in lamel graphite cast iron. Master Thesis, Sakarya University, Graduate School of Natural and Applied Sciences, Sakarya.

[15] Yenice, B. S. (2002). Heat treatings of gray cast irons and ductile cast irons. Master Thesis, Marmara University, Graduate School of Natural and Applied Sciences, İstanbul.

[16] Yakut, R. & Çiftçi, Ö. (2022). The effects of reinforcement with TaC on the microstructure and wear properties of lamellar graphite cast irons. European Journal of Technique (EJT), 12 (1): 77-81, DOI: 10.36222/ejt.1088994.

[17] Altuncu, E., & Esen S. G. (2015). Ultra high temperature ceramics: tantalum carbide (TaC). Journal of Aeronautics and Space Technologies (JAST), 8 (1): 67-74.

[18] https://nanografi.com/microparticles/tantalum-carbide-tac-micron-powder-purity-99-9-size-3-m/ (27.10.2022).

[19] https://www.karfo-endustriyel.com.tr/tr/cozumler/endustriyel-mikroskop-cozumleri/dokme-demir-metalografisi/gri-dokme-demir-olcumleri#:~:text=Gri%20d%C3%B6kme%20demirde%2C%20kat%C4%B1la%C5%9Fma%20olduktan,-d%C3%B6kme%20demir%20olarak%20da%20isimlendirilir. (29.10.2022).

[20] https://www.ktu.edu.tr/dosyalar/14_14_00_0e11d.pdf (27.10.2022).

[21] https://teknoloji.isparta.edu.tr/assets/uploads/sites/436/files/makine-basma-deney-foyu-09052022.pdf (28.10.2022).

[22] Akgül, B. (2018). An investigation of effect of tin (Sn) on microstructures and mechanical properties of gray cast iron. Master Thesis, Selçuk University, Graduate School of Natural and Applied Sciences, Konya.

[23] Çalık, A., Bıçaklı, E. E., & Zerentürk, O. (2022). Comparison of microstructural and mechanical properties of GG-25 cast iron produced by spinning and sand casting method. Journal of Cihannuma Technology Engineering and Natural Sciences Academy, 1 (1): 1-22, DOI:10.55205/joctensa.11202223.

[24] https://www.zhycasting.com/properties-and-characteristics-of-grey-cast-iron/ (28.10.2022).